

Neutron Diffraction Study of the Magnetic Properties of  $\text{MnBr}_2$ †

E. O. WOLLAN, W. C. KOEHLER, AND M. K. WILKINSON  
*Oak Ridge National Laboratory, Oak Ridge, Tennessee*

(Received January 6, 1958)

The antiferromagnetic structure of  $\text{MnBr}_2$  ( $T_N = 2.16^\circ\text{K}$ ) has been determined by single-crystal neutron diffraction measurements at temperatures down to  $1.35^\circ\text{K}$  and with magnetic fields (0-13 kilo-oersteds) applied to the sample. The antiferromagnetic structure appeared to have hexagonal symmetry in the absence of a magnetic field but this was found to be associated with a structure domain-growth property. The true magnetic structure was found to be associated with one or another of three hexagonal axes, the particular growth direction being determined by the direction of an applied magnetic field. Information relating to indirect magnetic exchange *via* the bromine ions in this crystal was obtained from a study of the domain growth properties. The antiferromagnetic ordering transition in this compound was found to be nearly first order rather than of the usual second order type. A small lowering ( $\sim 2\%$ ) of  $T_N$  was observed for an applied field of 13.1 kilo-oersteds. Short-range order data were obtained from powder patterns.

## I. INTRODUCTION

MANGANOUS bromide crystallizes in the  $\text{CdI}_2$  layer-type hexagonal structure with one molecule per unit cell with the  $\text{Mn}^{++}$  ion at (000) and the two  $\text{Br}^-$  ions in  $\pm(\frac{1}{3}\frac{2}{3}u)$  with  $u=0.25$  and with  $a_0=3.868\text{ \AA}$  and  $c_0=6.272\text{ \AA}$ .

Measurements by Stout<sup>1</sup> have shown this compound to have a very pronounced specific heat anomaly at about  $2.16^\circ\text{K}$ , indicating a magnetic transition at this temperature.

Neutron diffraction measurements by the powder method were carried out about two years ago on this and a number of other layer-type compounds of the iron group which were shown to have layer-type antiferromagnetic structures with the moments aligned ferromagnetically within each hexagonal layer and with the spins in alternate layers oppositely aligned.<sup>2</sup> The powder pattern of  $\text{MnBr}_2$  was also consistent with this interpretation. In particular the most prominent magnetic reflection at  $2\theta \sim 5^\circ$  was indexable as (001) type. There was observed, however, in  $\text{MnBr}_2$  short-range order above the Néel temperature suggestive of antiferromagnetic ordering in the hexagonal layers, whereas in the other bromides and chlorides (except  $\text{MnCl}_2$ ) studied, this short-range order had a ferromagnetic character consistent with ferromagnetic ordering within the layers. On the basis of these differences and the possibility that other index assignments could be made to the close-in magnetic reflection, it was decided to make a single-crystal neutron diffraction study of this compound. The magnetic structure has now been found to be of a more complicated type than first proposed.

2. NEUTRON SPECTROMETER EQUIPMENT  
AND CRYSTAL PREPARATION

The neutron spectrometer with associated magnet and cryostat has been described previously.<sup>3</sup> Two

† Presented at the Pittsburgh Diffraction Conference, November 6-8, 1957.

<sup>1</sup> J. W. Stout [private communication (see reference 2)].

<sup>2</sup> See *Solid State Physics*, edited by F. Seitz and D. Turnbull (Academic Press Inc., New York, 1956), Vol. 2, p. 190.

<sup>3</sup> E. O. Wollan and W. C. Koehler, *Phys. Rev.* **100**, 545 (1955).

modifications have, however, now been made which are important for this investigation.

The first involved replacing the previously described magnet by one of more efficient design in which high current oil-cooled coils are used with their axes along the center line of the magnet poles shown in Fig. 1. With this magnet, fields up to 17 kilo-oersteds for a  $\frac{5}{8}\text{-in.}$  gap can be applied to the sample.

The second involved the development of a single-crystal goniometer device to operate at pumped helium temperatures. The constructional details of the cryostat with single-crystal goniometer are shown in Fig. 1. The crystal goniometer is inserted into the cryostat through the thin-wall central tube of the He container, and it ends up in a thin-wall Al end piece at the bottom of the cryostat. This end piece is sealed to the brass body of the He container by a pressure fit over a narrow annular contact area between the shoulder of the Al end piece and a  $45^\circ$  beveled surface at the bottom of the brass container. This pressure seal has been found very satisfactory for containing liquid He even below the  $\lambda$  point. The goniometer mechanism which holds the crystal is located in the Al container at the bottom of the inner cryostat and the liquid He surrounds the goniometer mechanism and the crystal. The gear wheel to which the crystal is attached can be rotated about a horizontal axis by another gear which is directly attached by a thin-wall tube to the knob at the top of the cryostat. One turn of this knob rotates the crystal  $60^\circ$ . The whole bottom assembly can be rotated about a vertical axis, the torque in this case being transmitted through the larger thin-wall tube which attaches at the top to a scale with a worm-gear drive. The shafts for transmitting the motions pass through O-ring seals at the top of the cryostat. By pumping on liquid He in this cryostat the lowest working temperature was about  $1.35^\circ\text{K}$ . Under these conditions a charge of He (1.8 liters) lasted about 15 hours.

The cryostat and magnet are mounted on the crystal table of the spectrometer which allows the magnetic

field to be placed along the scattering vector or at an angle with this vector in the scattering plane for a given crystal orientation. The usual BF<sub>3</sub> counter was used to count the scattered neutrons.

The MnBr<sub>2</sub> crystal used in this investigation was grown by slowly moving the material contained in a sealed quartz crucible through the heated region of a specially constructed furnace.<sup>4</sup> Several attempts were made before a satisfactory crystal was obtained. The best results seem to be obtained for crystals of this type if the inner walls of the crucible are coated with aquadag.

Since this material forms very soft crystals, care must be taken in the process of cutting them to the proper size. To this end, a thin circular aluminum template of the desired size ( $\frac{5}{16}$ -in. diam) was glued to a smooth cleavage plane of a rather large piece of the boule. A fine jeweler's saw was then used to cut a cylinder of the diameter of the template. The desired thickness was then achieved by cleaving thin layers from the back of this cylinder. The Al template was left in place and the cylinder was fitted into a thin-wall internally threaded (No. 80) cylindrical Al box into which was screwed a thin Al cover plate to hold the crystal firmly in place. This box, which was made with a small stud in its back, was firmly screwed in place in the center of the gear plate of the goniometer.

The crystal was thus mounted with the *c* axis horizontal and parallel to the axis of rotation of the gear. Any (*hkl*) plane can be brought into a vertical position by rotation about the horizontal axis. For convenience the orientations about this axis will be referred to as the angle  $\beta$ . After a given plane has been brought into the vertical position, it can be turned to the proper reflecting angle relative to the incident beam by rotation about the vertical axis within the cryostat. This orientation will be referred to as the angle  $\alpha$ , the angle  $\theta$  being reserved for the readings of the spectrometer table which orients the magnet and cryostat as a whole.

### 3. ANTIFERROMAGNETIC STRUCTURE

As was previously mentioned, the earlier powder data on MnBr<sub>2</sub> were first interpreted in terms of an antiferromagnetic sheet structure with the moments aligned ferromagnetically within each hexagonal layer and with oppositely directed spins in alternate layers, in which case the first strong magnetic reflection would be the (001) of a cell doubled along the *c* axis.

From the single-crystal measurements it was, however, quickly ascertained that this first magnetic reflection was not of the (001) type and later this was identified as an (*h0l*)-type reflection. Several other antiferromagnetic reflections of this type with different spacings were also observed and these were all found

<sup>4</sup> The single crystal of MnBr<sub>2</sub> was grown for us by J. J. Manning, Division of Applied Nuclear Physics, Oak Ridge National Laboratory.

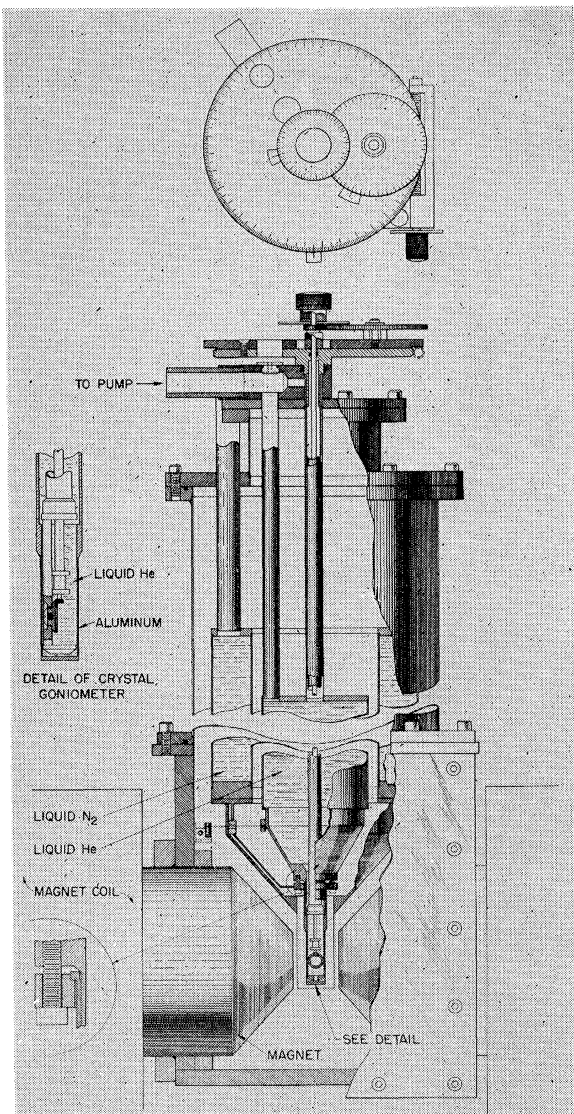


FIG. 1. Cryostat, single-crystal goniometer, and magnet pole pieces.

to have 120° symmetry about the *c* axis of the crystal. A concerted effort was then made to devise an antiferromagnetic array of moments which would account for the spacing and symmetry of the observed reflections. This met with no success, and it was not until effects on the reflected intensities of magnetic fields applied to the sample were investigated that the character of the antiferromagnetic structure became understandable.

It was observed that, if a magnetic field of about 1000 oersteds or greater was applied along the scattering vector of a given (*h0l*)-type reflection, the intensity of that reflection increased by about a factor of three and, if this field was then turned off, most of this increase of intensity remained frozen in. It was also observed that, after the intensity had been frozen in for a

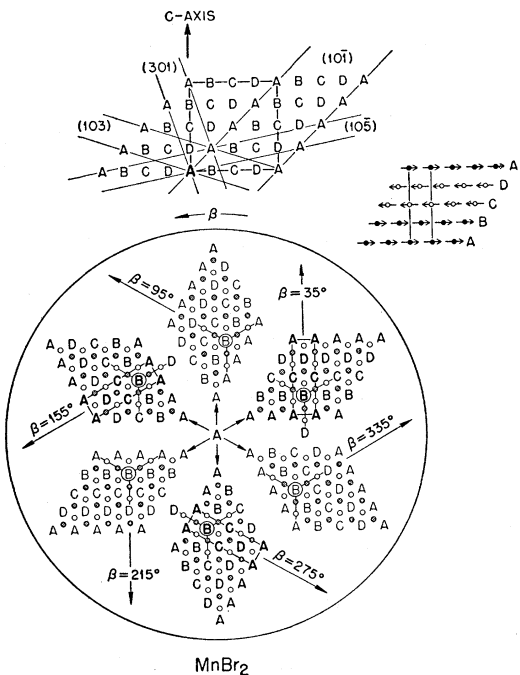


FIG. 2. The upper part of this figure shows the projection of the magnetic cell on a plane perpendicular to a [100] hexagonal direction. The lower part shows the hexagonal layers for the six possible directions of domain growth. The bolder regions represent the actual domain-growth directions. Two layers of bromine ions above the plane of metal atoms are shown by the open and shaded circles. The upper right-hand corner shows the actual spin assignments. Other features are discussed in the text.

particular  $(h0l)$  reflection, all other  $(h0l)$ -type reflections for a given value of the angle setting  $\beta$  of the goniometer, e.g.,  $\beta = 35^\circ$ , possessed about the same permanent increase in intensity, a factor of about three, over their original no-applied-field values. It was then further observed that the other sets of  $(h0l)$ -type reflections at  $120^\circ$  intervals ( $\beta = 155^\circ$  and  $\beta = 275^\circ$ ) around the  $c$  axis were essentially extinguished. It thus became evident that the antiferromagnetic structure did not possess threefold symmetry about the  $c$  axis of the crystal but only a onefold axis, which in the absence of an applied magnetic field could grow with equal probability along any one of three hexagonal directions. There is thus indicated a type of antiferromagnetic domain growth in this compound, the nature of which is different from that normally associated with this term in that it involves not only the orientation of spins within the structure but the direction of growth of the antiferromagnetic structure as well. The domain properties of this system and their behavior under applied magnetic fields will be discussed in more detail in the following section. For the purposes of determining the antiferromagnetic structure, it was necessary to determine the structure of a single domain. The fact that in this compound the crystal could be permanently prepared below  $T_N$  as a single antiferro-

magnetic domain was a simplifying factor in the determination of the magnetic structure.

In determining the indices of the crystal reflections, the powder data were used to ascertain the counter setting (20) for a given reflection in those cases where resolved magnetic peaks had been observed. When the crystal was so adjusted as to bring intensity into the counter at a given  $2\theta$ , the counter was scanned over the peak to obtain the optimum  $2\theta$  value for the reflection. This gives a check on the spacing value for the reflection.

From the spacing values and the crystal orientation of the most intense reflections, which were determined to be of the  $(h0l)$  type, it was possible to obtain the projection of the unit cell on a plane perpendicular to an  $[h00]$  direction.

The orientation of some of the observed  $(h0l)$ -type reflecting planes are shown in the upper part of Fig. 2.<sup>5</sup> At this stage of the magnetic structure determination there was no information available on the orientation of the spins of the various manganese atoms relative to the crystal axes, and it was necessary to make deductions on the basis of phase relationships only. Since the smallest-angle reflection which was observed indexed as  $(10\bar{1})$  on a hexagonal cell  $4 \times 4 \times 4$  times larger than the chemical cell, it was logical to assume that these planes passed through atoms of like spin orientation. The spins (or phases) of these atoms were thus labeled  $A$ , and correspondingly it was assumed that the intervening atomic layers were also of like spin and these were labeled  $B$ ,  $C$ , and  $D$ . It should be noted that this figure represents the projection of atoms on the plane, atoms  $B$  and  $D$  being in a different plane than atoms  $A$  and  $C$ . From the characteristics of the cell represented by this figure, it became possible to predict the presence or absence of certain  $(h0l)$  types of reflections. It is interesting to note from the figure that planes of index  $(101)$ ,  $(103)$ ,  $(10\bar{5})$ , etc. are of a different type than those of index  $(101)$ ,  $(103)$ ,  $(10\bar{5})$ , etc. since the former pass through  $A$ - and  $C$ -type atoms. As will be seen, reflections are observed only for planes of the latter type. This fact has significance not only for the antiferromagnetic structure of a single domain but also for the domain properties associated with the structure. It is also to be noted that all  $(h0l)$  planes for which reflections are observed have the same structure factor since, as can be seen from the figure, they correspond to spacings which always have the spin sequence  $ABCPA$ .

Having thus determined certain properties of the magnetic cell from reflections of the  $(h0l)$  type, it is necessary to show the other cell dimension from the more general  $(hkl)$  type of reflections. The results up to this point are suggestive of a cell having a spin arrangement in the hexagonal layers corresponding to that shown in, for example, the upper right-hand

<sup>5</sup> Figure 2 was drawn such that the first reflection indexes as  $(10\bar{1})$ . Since it could equally well be made a  $(101)$  reflection, no distinction will be made except where it is specifically required.

section of the lower part of Fig. 2. If this is the proper spin phase arrangement, the antiferromagnetic structure is obviously not hexagonal. It can be conveniently represented by an orthorhombic cell for which the  $a$  and  $b$  axes are outlined in Fig. 2 in the hexagonal layers. Although we have chosen an orthorhombic cell, the antiferromagnetic structure is of lower symmetry.

The reflections (indexed on the basis of the orthorhombic cell) for which intensities were observed are listed in the first column of Table I, and these reflections agree in angle of orientation and spacing value with the orthorhombic cell which was referred to in connection with Fig. 2 and for which a half of the cell is represented by the atoms outlined by dashed lines in Fig. 3. It should be noted that the magnetic cell determination depends also on the fact that no intensity was observed for reflections of the  $(101)$ , etc. type. Note also that the orthorhombic indices are the same as for hexagonal indexing in the case of  $(h0l)$ -type reflections.

The second step in obtaining the actual antiferromagnetic structure involves a determination of the orientation of the spins relative to the axes of the crystal. This can be obtained on the one hand from a determination of the relative intensities of the various reflections, which are dependent on the values of  $q^2 = 1 - (\mathbf{e} \cdot \mathbf{S})^2$  where  $\mathbf{e}$  is the unit scattering vector and  $\mathbf{S}$  is a unit vector parallel to the atomic spin vector, the assumption being made in this representation that all spins are parallel or antiparallel to a single direction in the crystal. To make significant relative intensity measurements on the magnetic reflections, it was first required that a check be made of the importance of absorption and extinction in the crystal. To do this, several nuclear reflections were studied and it was found that, for  $\text{MnBr}_2$  crystals of the size used, neither absorption nor extinction has a significant effect on the observed relative intensities. The intensities of the magnetic reflections, as determined without any correction for these effects, are tabulated in Column 5 of Table I.

TABLE I. Magnetic structure data.<sup>a</sup>

Orthorhombic $hkl$	$2\theta$	$\varphi$	$q^2$	$F_{\text{obs}}^2$ (barns)	$70\% \text{ sat.}$ $F_{\text{calc}}^2$ (barns)
1 0 $\bar{1}$	5° 14'	61° 56'	1	0.56	0.61
1 0 3	8° 42'	31° 58'	1	0.54	0.56
1 0 $\bar{5}$	13° 8'	20° 30'	1	0.44	0.50
1 0 7	17° 52'	14° 44'	1	0.35	0.39
3 0 1	14° 4'	79° 54'	1	0.49	0.47
3 0 $\bar{3}$	15° 42'	61° 52'	1	0.41	0.42
3 0 5	18° 36'	48° 15'	1	0.39	0.36
3 0 $\bar{7}$	22° 12'	51° 19'	1	0.35	0.30
1 1 1	16° 48'	81° 34'	0.07	0.028	0.039
1 1 $\bar{3}$	18° 12'	66° 1'	0.31	0.092	0.085
1 1 5	20° 44'	53° 26'	0.35	0.110	0.126
1 1 $\bar{7}$	24° 4'	46° 4'	0.45	0.130	0.169
3 1 $\bar{1}$	21° 20'	83° 21'	0.43	0.134	0.134

<sup>a</sup> Here  $\varphi$  is the angle between the normal to the plane and the  $c$  axis.

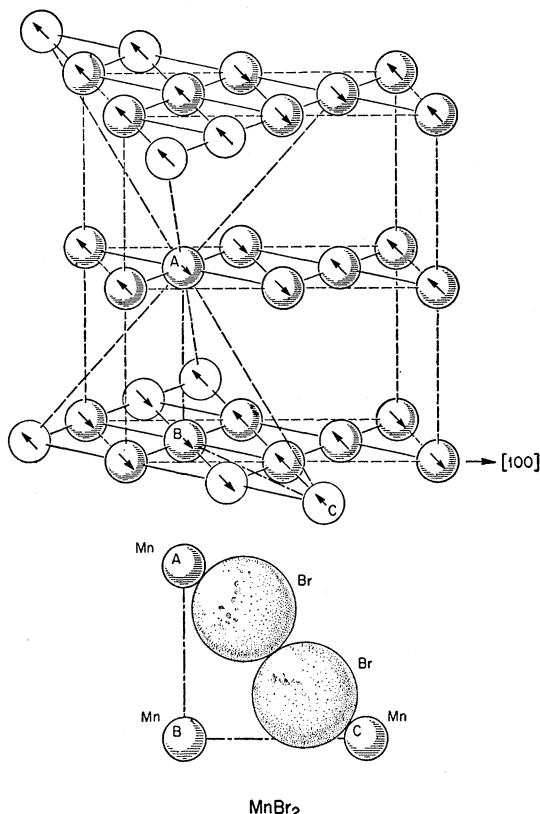


FIG. 3. Upper part of figure shows half of the orthorhombic antiferromagnetic cell. The radial lines indicate antiferromagnetic coupling along lines of bromine ions, as shown in the lower part of figure.

At the moment these values are to be considered on a relative basis only. These relative intensities are in good accord with corresponding values (Column 6, Table I) calculated on the basis of the spins being parallel to the short axis ( $b$  axis) of the orthorhombic cell, the  $b$  axis being parallel to an  $[h00]$  direction in the hexagonal layers. This point is further verified (see next section) by magnetic field measurements made on the crystal prepared as a single antiferromagnetic structure domain.

The third step in determining the antiferromagnetic structure involves the identification of the spin orientation sequence associated with the letters  $ABCD$  which up to now have been used to identify the various spins in the cell. To do this, it was necessary to make absolute intensity measurements of the magnetic reflections. This was done by determining these intensities relative to those of a number of nuclear reflections for which the absolute scattering power could be directly deduced from the known coherent neutron scattering cross sections of manganese and bromine. This requires, however, that the parameters of the bromine-ion positions in the crystal be accurately known. A check of several nuclear reflections involving different bromine-ion contributions gave good con-

sistency on the basis of the listed bromine parameter  $u=0.25$ . These measurements thus gave the instrumental constants from which the intensities of the magnetic reflection could be determined on an absolute basis. The absorption correction, being small and having been shown to be rather insensitive to crystal orientation, drops out in a comparison of nuclear and magnetic reflections in the same sample. There is, however, an additional factor involved in the absolute intensity determination; namely, the degree of saturation of the spin system. It is to be expected in the first place that the  $Mn^{++}$  ion will have a magnetic moment associated with a spin only value of  $\frac{1}{2}$ . The low Néel temperature in this compound, however, makes it impossible to attain saturation of the spin system at the lowest temperature ( $1.35^{\circ}\text{K}$ ) reached in this experiment. A reasonable estimate, however, based on the temperature saturation curve of Fig. 7, would suggest that one is within about 20%<sup>6</sup> of saturation at  $1.35^{\circ}\text{K}$ , and also the frozen-in field saturation of a single domain was found to be incomplete to  $\sim 10\%$ . To within a reasonable limit of accuracy, then, the intensity saturation can be expected to be about 30% higher than the measured values. The intensities of the various reflections listed in Column 5 of Table I are the measured absolute values at  $1.35^{\circ}\text{K}$  without correction for lack of temperature saturation. These intensities can then be compared with the calculated values listed in the last column of Table I, which have been reduced by 30% to take account of incomplete saturation. These calculations are based on the spin assignment shown in the upper right-hand corner of Fig. 2, in which the spins  $ABCD$  in each hexagonal layer have been taken in the sequence  $\uparrow\uparrow\downarrow\downarrow$  with the spin direction parallel and antiparallel to the short  $b$  axis of the orthorhombic antiferromagnetic cell. Half of the cell for this structure is shown in Fig. 3. It is evident that a smaller cell could be used to describe this structure, but indexing on the basis of the orthorhombic cell is somewhat simpler.

#### 4. DOMAIN STRUCTURE

When the  $MnBr_2$  crystal is lowered in temperature below the Néel point ( $2.16^{\circ}\text{K}$ ) in the absence of a magnetic field, it develops a threefold symmetry in its magnetic structure which, as has been inferred in the previous section, is associated with the formation of antiferromagnetic structure domains. These domains have been found to grow with equal probability along three of the hexagonal axes of the crystal. Most of the properties of these domains can be studied by the application of a magnetic field along the scattering vector of an  $(h0l)$  type of magnetic reflection. For convenience the strong (101)-type reflection has been used in most cases.

<sup>6</sup> A fit of the data of Fig. 7 to a Brillouin function (see Fig. 9) is in agreement with this estimate within the accuracy of the measurements.

When the crystal is brought to a low temperature in the absence of a field, and a particular set of (101) planes (at  $\beta=35^{\circ}$ , e.g.) is brought into position to reflect, the effect of applied magnetic field strength on the intensity of this reflection is represented by the data plotted in the upper curve of Fig. 4. For small fields there is at first no noticeable increase in intensity,\* but after some critical field has been reached, which for this reflection is of the order of 400 oersteds, there is an abrupt increase in intensity associated with this reflection which breaks off at something like three times the no-field value. If the field is then turned off, a major fraction of this increase in intensity remains frozen in. If, then, one now investigates the (101) type of reflections at  $120^{\circ}$  in  $\beta$  ( $\beta=155^{\circ}$  and  $275^{\circ}$ ) away from this position, which before the application of the field had intensities comparable to that at  $\beta=35^{\circ}$ , it is found that their intensities have dropped to essentially zero value. The fact that the crystal remains as a single antiferromagnetic domain after the field has been removed is undoubtedly related to the fact that there appears to be a definite energy associated with the structure domain reorientation, as evidenced by the requirement of a minimum field value to bring about the change. The fact that the over-all intensity increase was not exactly equal to three is evidence that the distribution of the domains among the three orientations was not exactly equal. It should also be pointed out that the very abrupt change in intensity shown in Fig. 4 is not always realized. When the crystal had already been prepared as a single domain,

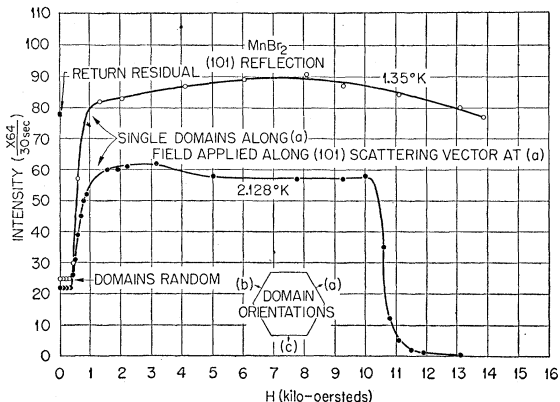


FIG. 4. Domain behavior and intensity changes as a function of applied magnetic field for two temperatures. The drop in the lower curve at 10.5 kilo-oersteds corresponds to point at which  $T=T_N(H)$ .

\* Note added in proof.—About the time this manuscript was submitted it was realized that a constructional feature of the goniometer could influence the magnetic field in the region of small fields. This feature involved a small annular vanadium bearing surface for the gear on which the crystal was mounted. Since vanadium becomes a superconductor at  $5.1^{\circ}\text{K}$ , the field in the vicinity of the gear on which the crystal is mounted would be reduced at low temperatures until the critical field ( $\sim 500$  kilo-oersteds) was reached. It is thus possible that the features of the field effects on  $MnBr_2$  at low fields would be modified if a nonsuperconducting bearing were used.

there seemed to be a washing out of the sharp break in the curve when the single domain was forced from one orientation to another.

Curves similar to that of Fig. 4 were also obtained for other reflections of the  $(h0l)$  type. Reflections of the  $(hkl)$  type were, however, found to disappear with the application of a field along their respective scattering vectors. This is readily accounted for on the basis that when the field direction is along the scattering vector of these planes, it is more optimally oriented to stabilize another domain direction than that associated with the particular  $(hkl)$  reflection in question.

It was shown in the previous section, on the basis of intensity measurements, that the spins are parallel to the short axis of the magnetic cell; i.e., parallel to a  $[100]$  hexagonal direction. It is thus of interest to determine the effectiveness of a magnetic field in reorienting the domains as a function of the angle of inclination of the field in the plane of the  $(101)$  scattering vector and the  $c$  axis. To do this the crystal was prepared, by initial field application, as a single domain oriented along, e.g.,  $\beta = 155^\circ$ . The  $(101)$ -type reflection at  $\beta = 35^\circ$  was then studied. The intensity was observed with no field and then in one case, for example, the crystal was tilted in  $\alpha$  angle to bring the field vector into the  $(00l)$  plane with  $\beta$  still equal to  $35^\circ$ , and a small field was applied and then turned off. The crystal was then returned to its  $(101)$  reflecting position and the intensity measured. This process was repeated for various field values, and for this case the results are represented by the upper curve of Fig. 5. Similar curves were then obtained with various orientations of the field vector  $H$  relative to the hexagonal plane of the crystal. Successive curves thus obtained are also shown in Fig. 5. An analysis of these data show that the field which is effective in orienting domains from one hexagonal axis to another is given by  $H_{\text{eff}} = H \cos y$ . This seems to be a reasonable result and it further substantiates the spin orientation assignment obtained from the relative intensity measurements discussed previously.

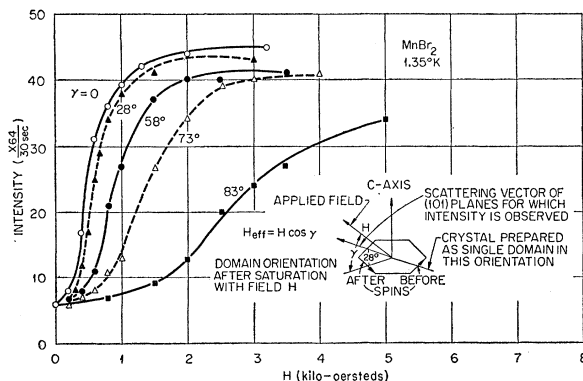


FIG. 5. Curves showing the effect of the magnetic field as a function of the angle  $\gamma$  of inclination with hexagonal layers. The field effective in flipping domains is  $H_{\text{eff}} = H \cos y$ .

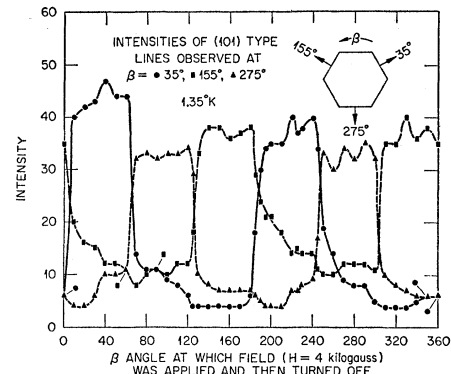


FIG. 6. Domain behavior as a function of angle  $\beta$  around the  $c$  axis at which magnetic field is applied.

Another domain study was made by determining the intensity associated with each of the three domain directions as a function of the angle  $\beta$  at which a magnetic field was applied. The measurements were made on a  $(101)$ -type reflection for which the scattering vector makes an angle of  $28^\circ$  with the hexagonal layers, and the magnetic field ( $H=4$  kg) was always applied at this same angle of inclination. The various  $(101)$ -type magnetic reflections appear at  $\beta = 35^\circ, 155^\circ$  and  $275^\circ$ . The field was applied at a given value of  $\beta$ , say  $30^\circ$ ; it was then turned on, and the intensities of the  $(101)$ -type reflections at all three  $\beta$  angles were then determined. This operation was then repeated with the field successively turned on and then off at other  $\beta$  orientations of the crystal. The resultant data are represented in Fig. 6. It is observed that a single domain direction is stable as long as the field is applied within a range of  $\beta$  of approximately  $30^\circ$  on either side of the direction of the scattering vector for the particular domain in question. The fact that the data show pronounced irregularities is not too surprising since the intensity measurements were made at the peak of the diffraction lines and the single crystal used in this study was by no means perfect, the observed line widths varying somewhat from one orientation to another.

Finally, there is one observation regarding the domain properties of this structure that has so far been passed over without comment. This property relates to the observation that these domains are found to grow along only three of the six hexagonal axes of the crystal. This situation is diagrammatically represented by the six domain patterns in the lower part of Fig. 2, in which the three observed directions of domain growth are represented by the bolder lines and the directions of no observed growth are more lightly represented. When only the magnetic manganese ions are considered, all six directions in the crystal are identical. It is thus suggested that the observed threefold symmetry of domain growth must be associated with the bromine ions in the crystal. As an aid in considering this point, two layers of bromine ions above the hexagonal sheet of metal atoms have been represented in Fig. 2. The

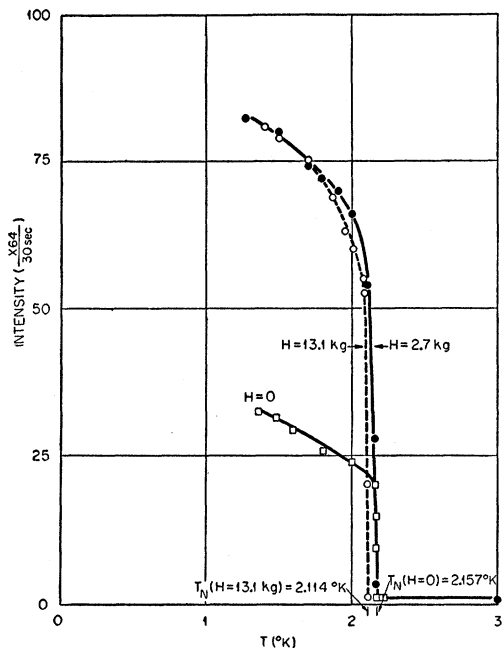


FIG. 7. Antiferromagnetic transition *versus* temperature and applied magnetic field. The squares ( $H=0$ ) correspond to three directions of domain growth, whereas circles ( $H>0$ ) correspond to growth of a single domain.

layer of  $\text{Br}^{++}$  ions at the positions  $(\frac{1}{3} \frac{2}{3} \frac{1}{4})$  of the chemical cell are represented by the open circles and those at  $(\frac{2}{3} \frac{1}{3} \frac{3}{4})$  are represented by the shaded circles. Inspection of the diagram shows that the bromine positions relative to the magnetic structure are different in a domain growth direction at, e.g.,  $\beta=35^\circ$  than in the directions  $60^\circ$  on either side of this direction; i.e.,  $\beta=95^\circ$  or  $335^\circ$ . To determine the particular directions in the crystal which relate the bromine positions to the directions of magnetic domain growth requires that the  $\beta$  angles and the intensities of a series of nuclear reflections of the (101) type (chemical cell) be correlated with the  $\beta$  angles of the observable magnetic domains. Data of this type were obtained and used in constructing the domain diagram of Fig. 2. These nuclear (101)-type reflections are alternately weak and strong as one progresses by  $60^\circ$  steps around the  $c$  axis of the crystal.

The implications of the dependence of the directions of domain growth on the bromine ion positions will be considered in the later section on magnetic coupling.

##### 5. ORDERING TRANSITION—EFFECT OF MAGNETIC FIELDS

The intensity of the single-crystal reflections from a (101)-type plane as a function of temperature and also of applied magnetic fields in the pumped He region is shown in Fig. 7. The open squares represent the intensity in the absence of a magnetic field. It is evident from the shape of this curve that the temperature dependence of the magnetic ordering is not of the Brillouin type; in fact the very sharp rise near the Néel

temperature indicates a transition of nearly first order rather than of the usual second-order type. The temperatures in these experiments were determined from measurements of the He vapor pressure and by the use of a calibrated carbon resistor. The absolute temperature is probably not accurate to more than a few millidegrees.

When the transition data are obtained with a small field ( $H=2.7$  kilo-oersteds) the same general type of curve is obtained, but in this case the intensity rises to about three times the no-field value. From the discussions in previous sections it is now evident that this increase with applied field arises from the fact that the intensity is distributed among three domains in the absence of a field, whereas with the field the domains are brought into a single orientation.

When the strength of the magnetic field applied to the sample is increased, it is observed that the Néel temperature is lowered over the no-field value. This is shown for the maximum field of 13.1 kilo-oersteds in Fig. 7. The dependence on magnetic-field strength is shown in more detail in Fig. 8.

Another representation of the field dependence of the antiferromagnetic transition is given in Fig. 4. The upper curve which represents the intensity of a (101)-type reflection as a function of magnetic field for an initially random orientation of magnetic domains shows only a small decrease of intensity at the maximum value of applied field. This curve was taken at  $1.35^\circ\text{K}$ . The lower curve which was taken at a temperature of  $2.128^\circ\text{K}$  shows a very different behavior in that the intensity falls to zero at a field of about 10.5 kilo-oersteds. Reference to Fig. 8 shows that this is just the value of the magnetic field for which the corresponding Néel temperature becomes equal to the temperature of the sample, and hence for fields above this value no order is to be expected.

Let us consider now what may be the cause of the

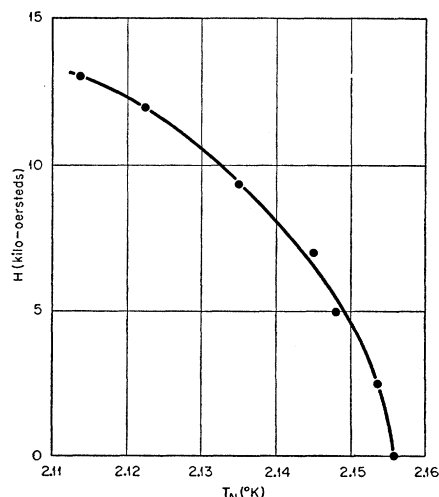


FIG. 8. Néel temperature *versus* applied magnetic field.

first-order character of the antiferromagnetic transition in MnBr<sub>2</sub>. Magnetic transitions of this type have previously been observed, as far as we know, only in cases where a crystallographic phase change takes place in the region of the ordering temperature. Such a situation is readily accounted for on the basis of an increase in the exchange coupling associated with the change in structure. Since the phase change is of first order, the magnetic transition could then also be of this type.

In the case of MnBr<sub>2</sub>, where no such phase change takes place, some other method of effecting the sudden rise in moment value must be sought.<sup>7</sup> It seems that the first-order type of transition in this case is in some way associated with the domain character of the antiferromagnetic structure.

Let us consider first the situation at low temperatures where long-range order has already developed. When once developed, the long-range order associated with the three directions of domain growth can be considered to be independent of each other and a two-sublattice molecular field picture for each of these directions should be approximately valid. The approach to saturation for  $T < T_N$  would thus be expected to follow a Brillouin-type function, but this would be the function for which the onset of long-range order should have occurred at some higher temperature  $T_{N'}$  rather than the observed  $T_N$ . The lower experimental curve ( $H=0$ ) of Fig. 7 has the shape to satisfy this condition. Figure 9 shows the adjusted location of the experimental transition data fitted to a Brillouin-type curve. Since the data represent neutron intensities, the fit is made to  $B^2(a)$ . The data and the curve thus suggest that the effective exchange coupling in the region of long-range order is related to a  $T_{N'} \approx 3^\circ\text{K}$  rather than the directly observed transition temperature  $T_N = 2.16^\circ\text{K}$ . The equivalent exchange field for this case ( $S=\frac{5}{2}$ ) is thus given by  $H_{\text{exh}} \approx (k/\mu)T_{N'} = 9$  kilo-oersteds.

We consider now the question as to why the ordering transition is suppressed from  $T_{N'}$  to  $T_N$ . It is evident that in the region of  $T > T_N$  where only short-range order can develop that a two-sublattice model is unsatisfactory. Owing to the possibility of structure domain growth along any one of three equivalent hexagonal axes, a given spin is subjected to ordering forces which are not simply related to the exchange forces present in the ordered state. Qualitatively, it is to be expected that the tendency for ordering along any one of three directions will result in reduction of the effective exchange force over that observed for the ordered state. This tendency might thus be expected to effect a reduction in the ordering temperature in a fashion somewhat similar to that associated with a crystal phase change since, once ordering has abruptly

<sup>7</sup> The situation encountered here may be very similar to order-disorder transitions in  $AB_3$ -type alloys, which are of first order and which have been accounted for theoretically. See F. C. Nix and W. Shockley, Revs. Modern Phys. 10, 1 (1938).

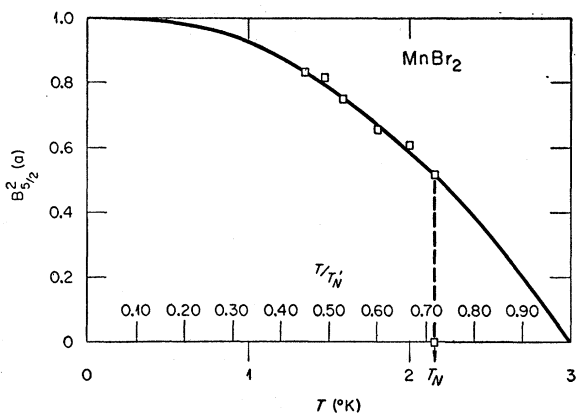


FIG. 9. Antiferromagnetic transition data ( $H=0$ ) fitted to a Brillouin function.

set in, each domain becomes a separate entity and the normal exchange becomes effective.

Let us return now to the observed effect of magnetic fields on the ordering temperature  $T_N$ . It was observed that a field of 13 kilo-oersteds, which is of about the same magnitude as the exchange field, reduces  $T_N$  by only about 2%. This small effect is undoubtedly associated with the fact that the field was always applied perpendicular to the direction of spin orientation. This direction of field application was dictated by the fact that (a) a given domain growth direction is stable only for fields applied in the range of  $30^\circ$  on either side of the perpendicular to the spin directions and (b) the fact that the present apparatus did not allow the field to be applied at large angles with the scattering vector of the reflecting planes to be studied.

Under the conditions of the experiment in which the field was applied perpendicular to the spin directions, it is found on the basis of simple molecular field considerations, neglecting anisotropy forces, that the energy associated with the ordered spin system is independent of the applied magnetic field. The observed small effect of the field on  $T_N$  can thus be accounted for only on the basis of a more refined theory including effects associated with some form of anisotropy energy. Although simple molecular field theory does not predict a change of  $T_N$  with applied field, it does predict a decrease with field of the observed intensity of the antiferromagnetic superlattice reflections; i.e., the approach to paramagnetic saturation. The upper curve of Fig. 4 and similar curves taken with powder samples indicate a decrease of intensity at high fields which is undoubtedly to be associated with the paramagnetic saturation effect.

## 6. SHORT-RANGE ORDER

In powder patterns taken above the Néel temperature in the liquid He region very pronounced short-range order peaks are observed at the position at which the strong (101) magnetic reflection develops at lower

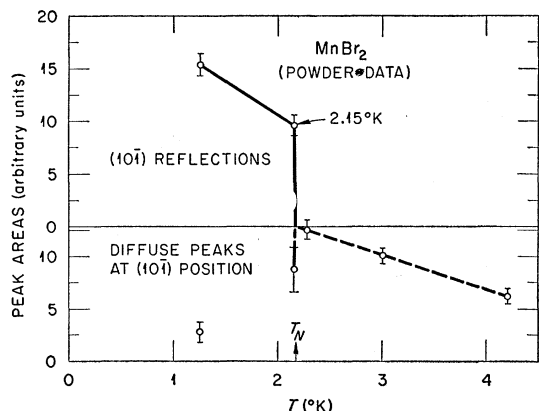


FIG. 10. Powder-data temperature dependence of  $(10\bar{1})$  magnetic reflection and associated short-range-order peak.

temperatures. It is only the width of these diffuse peaks ( $\sim 2.5^\circ$  at half maximum) that allows one to distinguish them from true Bragg reflections ( $\sim 1.5^\circ$  wide at half max).

The growth of short-range order as one approaches the Néel temperature in  $\text{MnBr}_2$ , as represented by the area of the diffuse peaks, is shown in Fig. 10 for  $T > 2.16^\circ\text{K}$ .

Below the Néel temperature the powder data show the sudden onset of order by the growth of the coherent  $(10\bar{1})$  reflections, as represented in the upper part of Fig. 10. These data are in good accord with the more detailed single-crystal results shown in the lower curve of Fig. 7. These Bragg peaks are superposed on diffuse peaks of about the same width as the isolated peaks observed for  $T > T_N$ . It is difficult to separate the diffuse peaks from the true Bragg reflections since these are also quite broad. The results, however, are sufficiently good to indicate the first order fall-off character of the diffuse peak accompanying the first-order increase in the coherent reflection. These points were taken at a temperature of  $2.15^\circ\text{K}$  which is just below  $T_N$ .

## 7. MAGNETIC COUPLING

In a compound such as  $\text{MnBr}_2$ , where the manganese ions are well separated from each other, any magnetic exchange between these ions must be of an indirect type *via* the intervening bromine ions. Although the over-all picture of magnetic coupling in a relatively complicated situation of this type would be very difficult to interpret in even a qualitative way, some interesting points in this regard have come from the study of the domain characteristics of the system. These are related to the observation that the domain growth follows only three of the six hexagonal directions in the crystal, all of which are identical for the manganese ions. The relation of the bromine ions to these six directions are shown in projection on the hexagonal

planes in Fig. 2. Consider in the domain at  $\beta=35^\circ$ , e.g., the circle drawn around the  $B$  atom in the layer. This circle is drawn to represent the  $A$  atom in the next hexagonal layer of metal atoms above the plane of the paper. The three lines radiating out from this circle represent lines which join the  $A$  atom in the upper plane to metal atoms in the plane of the paper. These lines pass nearly through the centers of adjacent bromine ions in intervening layers. A three-dimensional representation of these radial lines is given in connection with the diagram of the structure in Fig. 3. It can be seen in this figure that the central  $A$  atom is joined by these lines to six metal atoms in adjacent layers and that five of these atoms have opposite spin orientation to that of the central atom and one has like orientation. The disposition of the bromine ions along these lines is shown in the lower part of this figure. At an angle in the crystal in which the domains are found to grow, this particular set of bond directions, which involves a nearly straight line connection between manganese and bromine ions, is then to be associated with a preponderance of antiferromagnetic exchange. Now, for comparison, if one looks at a direction in the crystal in which domain growth is not observed, e.g.,  $\beta=95^\circ$  in Fig. 2, one observes that the orientation of the radial lines relative to the corresponding domain growth direction is different than in the previous case; and from a study of the arrangement one can readily determine that in this case a central  $A$  atom would have a predominance of ferromagnetic coupling along the specified bond directions, there being five ferromagnetic and only one antiferromagnetic relationship to the central atom.

The data thus suggest that indirect antiferromagnetic exchange coupling along nearly linear  $\text{Mn}^{++}-\text{Br}^--\text{Br}^--\text{Mn}^{++}$  bond linkages are of significance in determining the antiferromagnetic structure in  $\text{MnBr}_2$ . The fact that this two-anion indirect exchange appears to be antiferromagnetic might be expected by analogy with the single-anion superexchange mechanism.

It is evident in the case of  $\text{MnBr}_2$  that other significant contributions to magnetic coupling must also exist, because the most optimum structure for the above type of indirect exchange would be for all six linkages between layers to be antiferromagnetic. If this were the case, an antiferromagnetic layer structure would have developed. This would also be true if the intralayer coupling were ferromagnetic. It would thus appear that some antiferromagnetic intralayer coupling is required to stabilize the  $\text{MnBr}_2$  magnetic structure.

## 8. ACKNOWLEDGMENTS

The authors are indebted to H. R. Child for assistance with the measurements, to D. E. LaValle for preparing the pure compound, and to J. J. Manning for growing the single crystals.

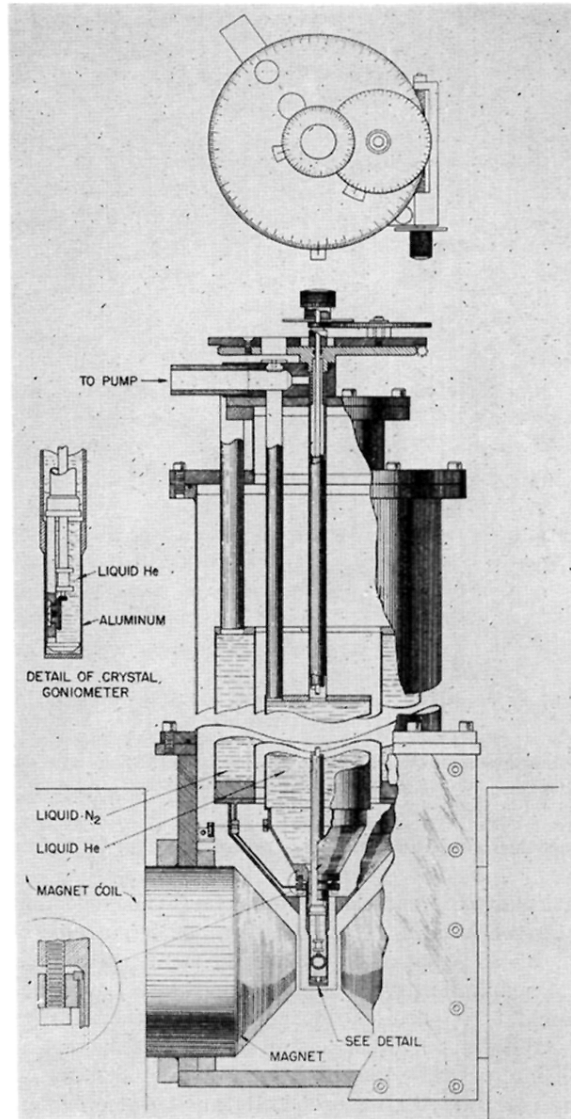


FIG. 1. Cryostat, single-crystal goniometer, and magnet pole pieces.